TECH LIBRARY KAFB, NM
0060517

NASA CONTRACTOR REPORT

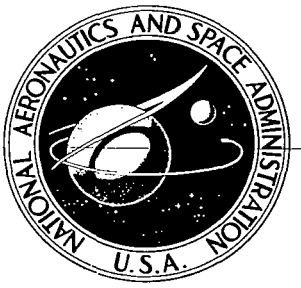

NASA CR-136
c. 1

LOAN COPY: RETURN TO
AFWL (WLIL-2)
KIRTLAND AFB, N MEX

NASA CR-1362

COMMENTS ON THE NATURE OF THE OUTSIDE BOUNDARY LAYER ON A LIQUID SPHERE IN A STEADY, UNIFORM STREAM

by Brice S. Sumner and Franklin K. Moore

Prepared by
CORNELL UNIVERSITY
Ithaca, N. Y.
for Lewis Research Center

NATIONAL AERONAUTICS AND SPACE ADMINISTRATION • WASHINGTON, D. C. • MAY 1969

TECH LIBRARY KAFB, NM
0060517
NASA CR-1362

COMMENTS ON THE NATURE OF THE OUTSIDE BOUNDARY LAYER ON A LIQUID SPHERE IN A STEADY, UNIFORM STREAM

By Brice S. Sumner and Franklin K. Moore

Distribution of this report is provided in the interest of information exchange. Responsibility for the contents resides in the author or organization that prepared it.

Prepared under Grant NGR-33-010-042 by
CORNELL UNIVERSITY
Ithaca, N.Y.

for Lewis Research Center

NATIONAL AERONAUTICS AND SPACE ADMINISTRATION

For sale by the Clearinghouse for Federal Scientific and Technical Information
Springfield, Virginia 22151 – CFSTI price $3.00

FOREWORD

The research described herein, which was conducted at Cornell University, Department of Thermal Engineering, was performed under NASA Grant NGR-33-010-042 with Dr. John C. Evvard, NASA Lewis Research Center, as Technical Monitor.

SUMMARY

An analytical and experimental investigation was made to determine in a qualitative way the nature of the boundary layer on the outside of a liquid sphere in a steady, uniform stream at high Reynolds number. The results indicate that the small perturbation boundary layers assumed by some authors are not justified when the densities and viscosities of the fluids inside the sphere and outside of it are comparable.

INTRODUCTION

A study of fluid dynamic confinement mechanisms may lead to an improved engineering capability for restraining very hot gases (as in nuclear and plasma devices) without the direct use of confining walls. An important consideration in such a study is the role of viscosity which is crucial in a completely encapsulated flow. The motion of a liquid drop in a surrounding fluid at rather high Reynolds number is a prototype of the flows of interest. Though the stabilizing mechanism of surface tension is available only for small scale flows, knowledge about the inner and outer boundary layers in these flows should be helpful in the study of more interesting self-contained flows.

This report, then, gives information about the nature of the boundary layer on the outside of a drop in a steady, uniform stream at large Reynolds number. The surface tension is assumed to be large enough to make the drop nearly spherical. Harper and Moore (Ref. 1) assumed that the velocity in the boundary layer on such a liquid sphere is given by a small perturbation of the inviscid flow around a solid sphere such that the velocity and tangential shear at the surface match those of an interior boundary layer in which the velocity is a small perturbation of Hill's inviscid spherical vortex solution. A typical velocity profile meeting this assumption is shown in figure 1. Harper and Moore assumed that this small perturbation scheme is applicable when the inside and outside densities and viscosities are comparable, but the results of this note indicate that under these conditions the velocity defect (the maximum deviation of the boundary layer velocity from the outside inviscid velocity at the surface) is $O(U_\infty)$, and that a linearization of the boundary layer equations made by assuming a small perturbation is not justified. The nature of the outside boundary layer is investigated here by: (1) examining the small Reynolds number Stokes-Oseen type of expansions for the liquid sphere at moderately large Reynolds numbers; (2) experiment; and (3) examining two terms of a power series in time for the impulsive start of the liquid sphere.

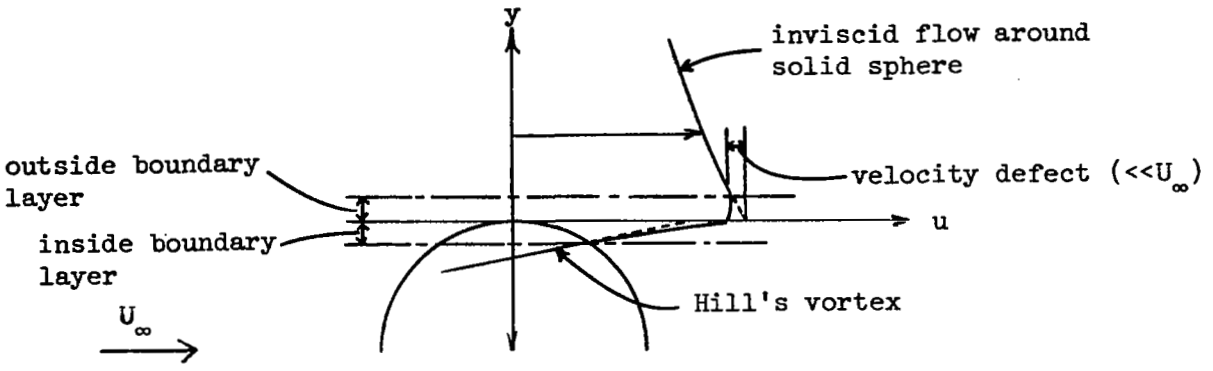

Figure 1. A typical velocity profile using the small perturbation assumption.

STOKES-OSEEN EXPANSION FOR LIQUID SPHERE

It is a fact (although possibly due to coincidence) that the Stokes-Oseen expansion of the stream function for uniform flow around a solid sphere at small Reynolds number (Proudman and Pearson (Ref. 3)) gives an accurate description of the actual flow behind the sphere at Reynolds numbers which are below that at which the wake vortices begin to shed, but which are still fairly large. Specifically, it accurately predicts the shape and size of the wake eddy behind the sphere (Van Dyke (Ref. 7) page 150). The comparable expansions for the liquid sphere given by Taylor and Acrivos (Ref. 6) are similarly used here at moderately large Reynolds numbers in the expectation that they will give at least qualitative information concerning the wake eddy, if any, behind the liquid sphere.

If we pick coordinates and velocities as shown in figure 2 and define stream functions such that

$$u^s = -\frac{1}{r\sin\theta}\,\psi^s_r \;,\quad \hat{u}^s = -\frac{1}{r\sin\theta}\,\hat{\psi}^s_r$$

$$v^s = \frac{1}{r^2\sin\theta}\,\psi^s_\theta \;,\quad \hat{v}^s = \frac{1}{r^2\sin\theta}\,\hat{\psi}^s_\theta \qquad (1)$$

then the two term small Reynolds number outside expansion valid near the sphere for ψ^s and the matching expansion inside the sphere for $\hat{\psi}^s$ are:

$$\psi^s = (\frac{1}{r} - mr + 2\ell r^2)(\frac{1}{4\ell} + \frac{Rm}{32\ell^2})\sin^2\theta + \frac{Rm\sigma}{160\ell^3}(1 - \frac{1}{r^2})\sin^2\theta\cos\theta$$

$$- \frac{Rm}{32\ell^2}(2\ell r^2 - mr + 1 - \frac{1}{r} + \frac{1}{r^2})\sin^2\theta\cos\theta + O(R^2) \tag{2}$$

$$\hat{\psi}^s = (r^4 - r^2)(\frac{\sigma}{4\ell} + \frac{Rm\sigma}{32\ell^2})\sin^2\theta +$$

$$\frac{Rm\sigma}{160\ell^3}(4 + 5\sigma)(r^3 - r^5)\sin^2\theta\cos\theta + O(R^2) \tag{3}$$

where R is the Reynolds number based on the radius and the outside viscosity, and $\sigma = \frac{\text{outside viscosity}}{\text{inside viscosity}}$, $\ell = 1 + \sigma$, $m = 3 + 2\sigma$. (4)

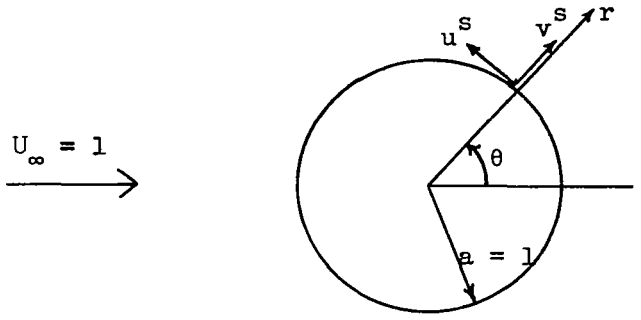

Figure 2. Notation for Stokes-Oseen expansion for a liquid sphere.

The theory does predict wake eddies for some ranges of R and σ. Wake eddies for various values of R and σ are shown in figure 3. Streamlines outside and inside the sphere for R = 100 and σ = 1.0 are shown in figures 4 and 5 respectively.

For a fixed Reynolds number the detached wake eddy of the liquid sphere goes smoothly into the attached wake eddy of the solid sphere as $\sigma \to 0$. Since the theory gives an accurate picture for σ = 0, there is some reason to hope that there is a range of σ for which it gives at least qualitative agreement with reality.

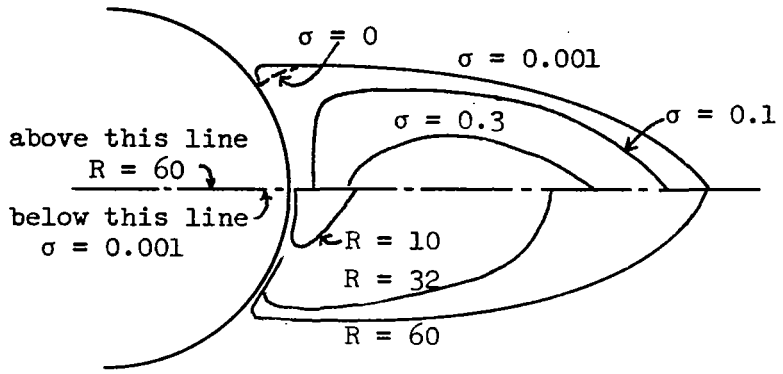

Figure 3. Sketch of wake eddies from Stokes-Oseen theory.

For the range of σ for which a wake eddy can exist the small perturbation boundary layer cannot be a good approximation since the inviscid flow around a sphere is then not an appropriate description of the outer flow. Further, the presence of the wake eddy implies separation of the boundary layer, and there is no mechanism that would cause the separation of a small perturbation boundary layer except in the vicinity of the rear stagnation point.

Two other interesting features predicted by this theory are the forward displacement of the center of motion of the inside flow shown in figure 5, and the absence of reverse eddies on the inside of the sphere. Both of these features were confirmed by the experiment below, and the former has been noted in Satapathy and Smith (Ref. 4), Magarvey and Kalejs (Ref. 2) and others.

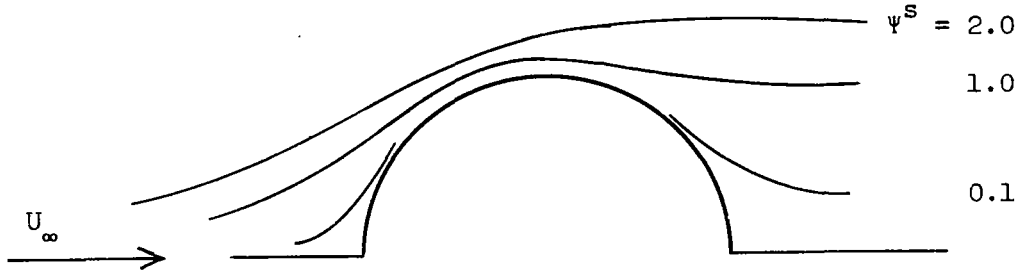

Figure 4. Sketch of the outside streamlines given by Stokes-Oseen theory. R = 100, σ = 1.

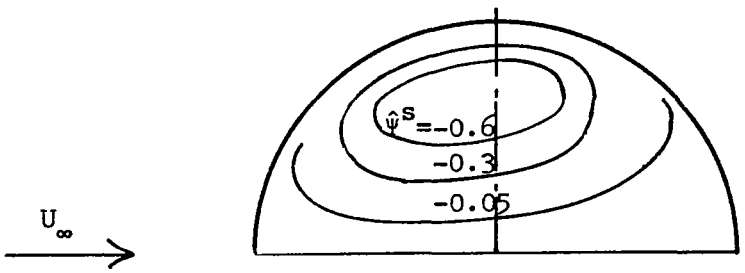

Figure 5. Sketch of the inside streamlines given by Stokes-Oseen theory. R = 100, σ = 1.

EXPERIMENT

A simple experiment was made to show the wake eddies and the internal circulation of drops. Drops of various liquids were formed at the bottom of a glass cylinder filled with a field solution of glycerin and water. The size of the drops was adjusted so that they rose at various Reynolds numbers below that at which they would follow a helical path. The lower half of the field solution was dyed. As a drop rose in the dyed solution, its wake eddy entrapped dyed fluid. Since the wake eddy is a closed, circulating region, it remained dyed, and thus was visible, as the drop traversed the clear field fluid. Circulation inside the drop itself was observed by introducing a thin mist of water droplets into the drop fluid. There was no flow inside drops which were small enough to be approximately spherical because the gradient in surface tension caused by surface active contaminants was strong enough to overcome the shearing force of the outside flow. Because of this it was necessary to use fairly oblate drops. These drops were large enough to have vigorous internal circulation, but their shape was a quantitatively unknown factor influencing the character of their wake.

The experiment demonstrated that for a large range of viscosity ratios the oblate drops had a wake eddy and a vigorous circulation inside the drop which contained no reverse eddies. The absence of reverse eddies within the drop tended to support the existence of a separation distance between the drop and its wake eddy although no separation could be distinguished (perhaps because of three dimensional effects and because the separation region is almost stagnant and would itself hold the dye for a long period of time). In a general way the experiment

tended to confirm the picture given by the Stokes-Oseen expansion. A point of disagreement was that the Stokes-Oseen expansion predicts that above $\sigma \approx 0.6$ no wake eddy will occur for any Reynolds number, but wake eddies were observed behind vigorously circulating oblate drops when $\sigma \approx 20$. Possibly shape is a stonger influence in triggering separation than is internal circulation in preventing it.

IMPULSIVE START OF A LIQUID SPHERE

By appealing to infinite surface tension one can conceive of the impulsive start of a liquid sphere. Although the impulsive start problem for such a body does not have any physical counterpart, its solution can still show the kinematic effect of the liquid sphere boundary conditions on the external flow. (These boundary conditions are continuity of velocity and tangential shear at the sphere surface). If, for example, the solution of the impulsive start problem for small time shows a detached wake eddy, this is a qualitative confirmation of the picture given at moderate Reynolds number by the small Reynolds number Stokes-Oseen expansion and further supports the argument against the applicability of the small perturbation boundary layer approximation for a certain range of σ.

We consider the flow field for small time and large Reynolds number around and in a liquid sphere accelerated impulsively at $t = 0$ from rest to a uniform velocity U_∞. At $t = 0+$ the inviscid flow outside the sphere will be the steady potential flow around a solid sphere in a uniform stream. What flow will be generated over the interior of the sphere at $t = 0+$ due to the impulsive acceleration? As soon as the motion begins, the flow in the interior, except right at the surface, must be irrotational because it was irrotational before the impulse, and the only source of vorticity is the sphere surface. Thus the inside flow field is describable by a potential, ϕ, and since $\nabla\phi \cdot$(surface normal vector) = 0 everywhere on the sphere surface, $\phi = 0$ everywhere inside at $t = 0+$.

Using the surface coordinates and the velocities shown in figure 6, and defining dimensional stream functions Ψ' and $\hat{\Psi}'$ such that

$$u' = \Psi'_{y'}, \quad v' = -\Psi'_{x'} - \frac{\cos\theta}{\sin\theta}\Psi' \tag{5}$$

$$\hat{u}' = \hat{\Psi}'_{y'}, \quad \hat{v}' = -\hat{\Psi}'_{x'} - \frac{\cos\theta}{\sin\theta}\hat{\Psi}'$$

the boundary layer equations in terms of the stream functions (Schlichting (Ref. 5) page 185) are:

$$\Psi'_{t'y'} + \Psi'_{y'}\Psi'_{x'y'} - (\Psi'_{x'} + \frac{\cos\theta}{a\sin\theta}\Psi')\Psi'_{y'y'} =$$

$$- \frac{1}{\rho'}P'_{x'} + \nu\Psi'_{y'y'y'} \tag{6}$$

$$\hat{\Psi}'_{t'y'} + \hat{\Psi}'_{y'}\hat{\Psi}'_{x'y'} - (\hat{\Psi}'_{x} + \frac{\cos\theta}{a\sin\theta}\hat{\Psi}')\hat{\Psi}'_{y'y'} =$$

$$- \frac{1}{\rho'}P'_{x'} + \hat{\nu}\hat{\Psi}'_{y'y'y'} \tag{7}$$

where the subscripts indicate differentiation, the primes mean dimensional quantities and the ^ symbol is used for quantities inside the sphere.

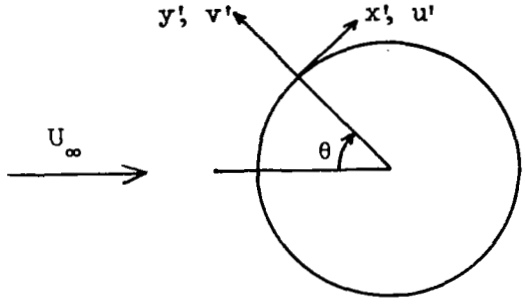

Figure 6. Notation for the impulsive start of a liquid sphere.

Because the motion is impulsive, the pressure gradients are given by:

$$- \frac{1}{\rho'}P'_{x'} = U'\frac{dU'}{dx'} = \frac{9U_\infty}{4a}\sin\theta\cos\theta$$

$$- \frac{1}{\hat{\rho}'}\hat{P}_{x'} = \hat{U}'\frac{d\hat{U}'}{dx'} = 0 \tag{8}$$

Using these gradients and the non-dimensional variables listed in (11), these equations become:

$$\Psi_{ty} - \Psi_{yyy} = \tau\left[\Psi_x \Psi_{yy} + \frac{\cos x}{\sin x}\Psi\Psi_{yy} - \Psi_y \Psi_{xy} + \frac{9}{4}\sin x\cos x\right] \tag{9}$$

$$\hat{\Psi}_{ty} - \frac{1}{\alpha^2}\hat{\Psi}_{yyy} = \tau\left[\hat{\Psi}_x \hat{\Psi}_{yy} + \frac{\cos x}{\sin x}\hat{\Psi}\hat{\Psi}_{yy} - \hat{\Psi}_y \hat{\Psi}_{xy}\right] \tag{10}$$

$$\left.\begin{aligned} &y = \frac{y'}{\sqrt{\nu t_o}}\ ,\ t = \frac{t'}{t_o}\ ,\ x = \frac{x'}{a}\ ,\ P = \frac{P' t_o}{\rho a U_\infty} \\ &\tau = \frac{U_\infty t_o}{a}\ ,\ \Psi = \frac{\Psi'}{U_\infty\sqrt{\nu t_o}}\ ,\ u = \frac{u'}{U_\infty}\ ,\ v = \frac{a^2 v'}{\nu t_o U_\infty} \\ &\sigma = \frac{\mu}{\hat{\mu}}\ ,\ \rho = \frac{\rho'}{\hat{\rho}'}\ ,\ \mu = \text{outside viscosity},\ \alpha = \frac{\sqrt{\sigma}}{\sqrt{\rho}} \\ &\rho' = \text{outside density},\ \nu = \frac{\mu}{\rho'}\ ,\ t_o = \text{an artificial time} \end{aligned}\right\} \tag{11}$$

The boundary conditions to be satisfied by these equations are the continuity of tangential shear and velocity at the interface and the matching of tangential velocity to the appropriate inviscid velocity at the outer edge of each boundary layer. Initially, in the outside boundary layer $\Psi_y = \frac{3}{2}\sin x$, and in the inside boundary layer $\hat{\Psi}_y = 0$.

In order to solve the boundary layer equations, we assume power series in τ for Ψ and $\hat{\Psi}$:

$$\Psi \sim \Psi^{(0)} + \tau\Psi^{(1)} + \cdots \tag{12}$$

$$\hat{\Psi} \sim \hat{\Psi}^{(0)} + \tau\hat{\Psi}^{(1)} + \cdots \tag{13}$$

The equations, initial conditions and boundary conditions for $\Psi^{(0)}$ and $\hat{\Psi}^{(0)}$ are:

$$\Psi^{(0)}_{yt} - \Psi^{(0)}_{yyy} = 0 \tag{14}$$

$$\hat{\psi}^{(0)}_{yt} - \frac{1}{\alpha^2}\hat{\psi}^{(0)}_{yyy} = 0 \tag{15}$$

$$\left.\begin{aligned} &\psi^{(0)}_{y}(x,o,t) = \hat{\psi}^{(0)}_{y}(x,o,t),\ \psi^{(0)}_{y}(x,\infty,t) = \frac{3}{2}\sin x,\ \psi^{(0)}_{y}(x,-\infty,t) = 0 \\ &\psi_{y}(x,y,o+) = \frac{3}{2}\sin x,\ \hat{\psi}^{(0)}_{y}(x,y,o+) = 0,\ \psi^{(0)}_{yy} \approx \frac{1}{\sigma}\hat{\psi}^{(0)}_{yy} \text{ at } y = 0 \end{aligned}\right\} \tag{16}$$

where the curvature terms in the tangential shear condition have been neglected consistent with the assumption of small time and large Reynolds number.

The solutions, which are easily obtained using Laplace transforms, are:

$$\psi^{(0)} = 3\sqrt{t}\,\sin x\left[(1-p)\eta\,\mathrm{erf}\,\eta + \frac{(1-p)}{\sqrt{\pi}}\left(e^{-\eta^2}-1\right) + p\eta\right] \tag{17}$$

$$\hat{\psi}^{(0)} = -\frac{3\sqrt{t}}{\alpha}\,p\sin x\left[\hat{\eta}\,\mathrm{erfc}\,\hat{\eta} - \frac{1}{\sqrt{\pi}}\left(e^{-\hat{\eta}^2}-1\right)\right] \tag{18}$$

where $p = \dfrac{\sqrt{\sigma\rho}}{1+\sqrt{\sigma\rho}}$, $\eta = \dfrac{y}{2\sqrt{t}}$, $\hat{\eta} = \dfrac{-\alpha y}{2\sqrt{t}}$

The equations, initial conditions and boundary conditions for $\psi^{(1)}$ and $\hat{\psi}^{(1)}$ are:

$$\psi^{(1)}_{yt} - \psi^{(1)}_{yyy} = \psi^{(0)}_{x}\psi^{(0)}_{yy} + \frac{\cos x}{\sin x}\psi^{(0)}\psi^{(0)}_{yy} - \psi^{(0)}_{y}\psi^{(0)}_{xy} + \frac{9}{4}\sin x\cos x = 9\cos x\sin x F(\eta) \tag{19}$$

$$\hat{\psi}^{(1)}_{yt} - \frac{1}{\alpha^2}\hat{\psi}^{(1)}_{yyy} = \hat{\psi}^{(0)}_{x}\hat{\psi}^{(0)}_{yy} + \frac{\cos x}{\sin x}\hat{\psi}^{(0)}\hat{\psi}^{(0)}_{yy} - \hat{\psi}^{(0)}_{y}\hat{\psi}^{(0)}_{xy} = 9\cos x\sin x\hat{F}(\hat{\eta}) \tag{20}$$

$$\left.\begin{aligned} &\psi_y^{(1)}(x,o,t) = \hat{\psi}_y^{(1)}(x,o,t),\ \psi_y^{(1)}(x,\infty,t) = \hat{\psi}_y^{(1)}(x,-\infty,t) = 0 \\ &\psi_{yy}^{(1)}(x,o,t) = \frac{1}{\sigma}\hat{\psi}_{yy}^{(1)}(x,o,t),\ \psi_y^{(1)}(x,y,0+) = \hat{\psi}_y^{(1)}(x,y,0+) = 0 \end{aligned}\right\} \quad (21)$$

To solve these assume that:

$$\psi^{(1)} = 9t^{3/2}\ \text{sinxcosx}f(\eta) \quad (22)$$

$$\hat{\psi}^{(1)} = 9t^{3/2}\ \text{sinxcosx}g(\hat{\eta}) \quad (23)$$

so that (19) and (20) reduce to:

$$f'''(\eta) + 2\eta f''(\eta) - 4f'(\eta) = -8F(\eta) \quad (24)$$

$$g'''(\hat{\eta}) + 2\hat{\eta}g''(\hat{\eta}) - 4g'(\hat{\eta}) = \frac{8}{\alpha}\hat{F}(\hat{\eta}) \quad (25)$$

where

$$F(\eta) = \frac{(1-p)^2}{\sqrt{\pi}}\eta e^{-\eta^2}\text{erf}\eta + \frac{(1-p)^2}{\pi}e^{-\eta^2}(e^{-\eta^2}-1) + \frac{p(1-p)}{\sqrt{\pi}}\eta e^{-\eta^2} - \frac{(1-p)^2}{4}\text{erf}^2\eta + \frac{1}{4}(1-p^2) - \frac{p}{2}(1-p)\text{erf}\eta \quad (26)$$

$$\hat{F}(\hat{\eta}) = -p^2\left[\frac{\hat{\eta}}{\sqrt{\pi}}e^{-\hat{\eta}^2}\text{erfc}\hat{\eta} - \frac{e^{-\hat{\eta}^2}}{\pi}(e^{-\hat{\eta}^2}-1) + \frac{1}{4}\text{erfc}^2\hat{\eta}\right] \quad (27)$$

The solutions for $f'(\eta)$ and $g'(\hat{\eta})$ are:

$$f'(\eta) = (1-p)\left[\left(\frac{1}{2} - \frac{1}{3\pi}\right)\operatorname{erfc}\eta - \left(1 + \frac{2}{3\pi}\right)\eta^2\operatorname{erfc}\eta\right.$$

$$\left. + \frac{2}{\sqrt{\pi}}\left(1 + \frac{1}{3\pi}\right)\eta e^{-\eta^2}\right] + (1-p)^2\left[\frac{2}{3\pi}\operatorname{erfc}\eta\right.$$

$$- \frac{1}{2}\operatorname{erfc}^2\eta + \frac{4}{3\pi}\eta^2\operatorname{erfc}\eta - \frac{1}{\sqrt{\pi}}\eta e^{-\eta^2}\operatorname{erfc}\eta$$

$$\left. - \frac{4}{3\pi}\left(1 + \frac{\eta}{\sqrt{\pi}}\right)e^{-\eta^2} + \frac{1}{\pi}e^{-2\eta^2}\right] \tag{28}$$

$$\alpha g'(\hat{\eta}) = p\left(\frac{1}{3\pi} - \frac{1}{2}\right)\left[\left(1 + 2\hat{\eta}^2\right)\operatorname{erfc}\hat{\eta} - \frac{2}{\sqrt{\pi}}\hat{\eta}e^{-\hat{\eta}^2}\right]$$

$$+ p^2\left[-\frac{2}{3\pi}\left(1 + 2\hat{\eta}^2\right)\operatorname{erfc}\hat{\eta} + \frac{1}{2}\operatorname{erfc}^2\hat{\eta}\right.$$

$$\left. + \frac{1}{\sqrt{\pi}}\hat{\eta}e^{-\hat{\eta}^2}\operatorname{erfc}\hat{\eta} + \frac{4}{3\pi}e^{-\hat{\eta}^2} - \frac{1}{\pi}e^{-2\hat{\eta}^2}\right] \tag{29}$$

Streamlines for the case $p = 0.1$ and $t' = .75\,\frac{a}{U_\infty}$ are sketched in figure 7. The detached wake eddy predicted by the small Reynolds number theory is present. However, it is obvious from expression (30) for the tangential velocity at the surface

$$u\big|_{y=o} = \frac{3p}{2}\sin x + \frac{3}{2}\left(\frac{3}{2} - \frac{1}{\pi}\right)p(1-p)t\tau\sin x\cos x + O(\tau^2) \tag{30}$$

that if only the first two terms of the series are considered, there will be a time when the eddy attaches to the sphere, and subsequently a reverse eddy forms inside the sphere. Using these first two terms of the series, the time that they predict reverse flow will start at the surface near the rear stagnation point is

$$t'_R = \frac{1}{\left(\frac{3}{2} - \frac{1}{\pi}\right)(1-p)}\,\frac{a}{U_\infty} \tag{31}$$

Thus $.846\,\frac{a}{U_\infty} < t'_R < \infty$, where the lower limit corresponds to a very viscous sphere. Consider a time less than $.846\,\frac{a}{U_\infty}$ but large enough so

that a wake eddy has formed at some p, and let $p \to 0$ (and hence $\sigma \to 0$). The wake eddy will move closer to the sphere until at $p = 0$ it attaches to the sphere. Consider a time (greater than $.846 \frac{a}{U_\infty}$) at which the wake eddy has just attached to the sphere at some $p \neq 0$. Then, for larger p the wake eddy is detached and for smaller p there is a reverse eddy inside the sphere which must disappear again as $p \to 0$. This inside reverse eddy does not appear in the small Reynolds number expansion, nor has it been observed in experiments. Possibly its appearance in the small time expansion is a result of that series not converging rapidly enough when $\tau \sim 1$ for the first two terms to give even a qualitatively correct picture of the flow.

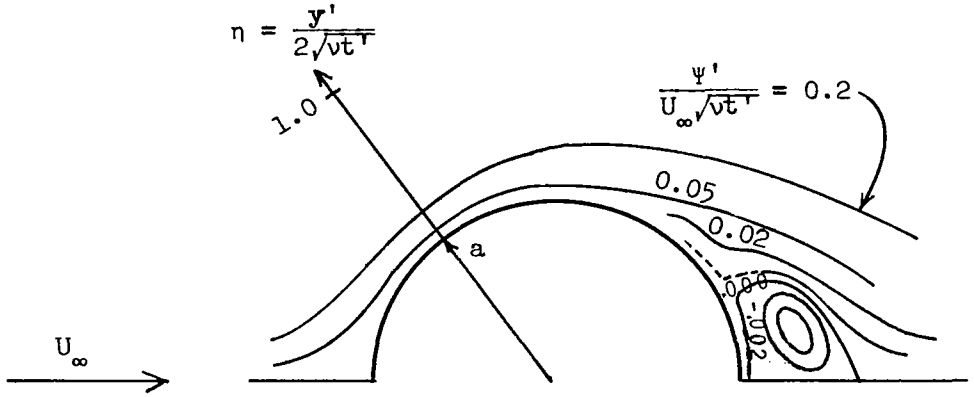

Figure 7. Streamlines for impulsive start of a liquid sphere. $t' = .75 \frac{a}{U_\infty}$, $p = 0.1$. (Radial scale outside of drop is magnified.)

Since the inviscid velocity at the outside edge of the boundary layer is $\frac{3}{2}\sin x$, the velocity defect in the outside boundary layer at small times $\sim \frac{3}{2}\sin x - \frac{3p}{2}\sin x = (1-p)\frac{3}{2}\sin x$. As time increases, this defect increases on the back hemisphere so that we can say the velocity defect predicted by this theory is at least $O(1-p)$. Thus, the small perturbation assumption cannot be valid, according to this theory, unless $p \not\approx 1$, which means that the product $\sigma\rho$ is large (the outside viscosity or density is much larger than that on the inside).

CONCLUSION

The three descriptions above of the nature of the outside boundary layer on a liquid sphere at moderate Reynolds numbers all say that there is a range of viscosity ratio for which the assumption of a small perturbation boundary layer is not realistic. The Stokes-Oseen expansion, when applied at moderate Reynolds numbers, indicates that the assumption is not good when $\sigma \leq O(1)$ (inside viscosity $\leq$ outside viscosity). The experiment indicated that it is not good for any liquid system in which the drop is fairly oblate. The two terms of the series solution of the impulsive start problem indicate that the small perturbation boundary layer can only be applicable, if at all, when $p \gtrsim 1$: that is, when inside viscosity << outside viscosity. Considering all three descriptions together, it seems likely that the liquid sphere has a normal kind of boundary layer on the outside when $\sigma \leq O(1)$.

Present work is directed toward obtaining a description of the inside boundary layer by impulsively turning on viscosity inside and outside of a Hill's vortex of arbitrary strength relative to a steady, uniform flow on the outside. It is hoped that the solution to this problem will indicate what strength the Hill's vortex must have in the steady case, and that it will also show any peculiarities of the boundary layer near the rear of the sphere where, presumably, it must separate and move forward along the sphere axis as a wake.

REFERENCES

1. Harper, J.F. and Moore, D.W.: The motion of a spherical liquid drop at high Reynolds number. J. Fluid Mech., Vol. 32, part 2, 1968, pp. 367-391.

2. Magarvey, R.H. and Kalejs, J.: Internal circulation within liquid drops. Nature, Vol. 198, 1963, pp. 377-378.

3. Proudman, I. and Pearson, J.: Expansions at small Reynolds numbers for the flow past a sphere and a circular cylinder. J. Fluid Mech., Vol. 2, 1957, pp. 237-262.

4. Satapathy, R. and Smith, W.: The motion of single immiscible drops through a liquid. J. Fluid Mech., Vol. 10, pp. 561-570.

5. Schlichting, H.: Boundary Layer Theory. Fourth Edition, McGraw-Hill Book Co., Inc., 1960.

6. Taylor, T.D. and Acrivos, A.: On the deformation and drag of a falling viscous drop at low Reynolds number. J. Fluid Mech., Vol. 18, 1964, pp. 466-476.

7. Van Dyke, M.: Perturbation Methods in Fluid Mechanics, Academic Press, 1964.

APPENDIX - SYMBOLS

a sphere radius

ℓ property parameter, $1 + \sigma$

m property parameter, $3 + 2\sigma$

p property parameter, $\frac{\sqrt{\sigma\rho}}{1 + \sqrt{\sigma\rho}}$

P dimensionless outside pressure, $\frac{P't_o}{\rho a U_\infty}$

P' outside pressure

$\hat{P}'$ inside pressure

R Reynolds number, $\frac{U_\infty a}{\nu}$

r radial distance

t dimensionless time, $\frac{t'}{t_o}$

t_o artificial time

t' time

u dimensionless outside velocity (tangential), $\frac{u'}{U_\infty}$

$\hat{u}$ dimensionless inside tangential velocity, $\frac{\hat{u}'}{U_\infty}$

u^s dimensionless outside tengential velocity, $\frac{u^{s'}}{U_\infty}$

$\hat{u}^s$ dimensionless inside tangential velocity, $\frac{\hat{u}^{s'}}{U_\infty}$

u' outside tangential velocity

$\hat{u}'$ inside tangential velocity

U_∞ free stream velocity

U' outside inviscid velocity at sphere surface

$\hat{U}'$ inside inviscid velocity at sphere surface

v dimensionless outside normal velocity, $\frac{a^2 v'}{\nu t_o U_\infty}$

$\hat{v}$ dimensionless inside normal velocity, $\frac{a^2\hat{v}'}{\nu t_o U_\infty}$

v' outside normal velocity

$\hat{v}'$ inside normal velocity

v^s dimensionless outside normal velocity, $\frac{v^{s'}}{U_\infty}$

$\hat{v}^s$ dimensionless inside normal velocity, $\frac{\hat{v}^{s'}}{U_\infty}$

x dimensionless tangential coordinate at sphere surface, $\frac{x'}{a}$

x' tangential coordinate at sphere surface

y dimensionless normal coordinate at surface, $\frac{y'}{\sqrt{\nu t_o}}$

y' normal coordinate at surface

α property parameter, $\frac{\sqrt{\sigma}}{\sqrt{\rho}}$

η outside similarity coordinate, $\frac{y}{2\sqrt{t}}$

$\hat{\eta}$ inside similarity coordinate, $-\frac{\alpha y}{2\sqrt{t}}$

θ angle between radial coordinate and axis of symmetry in radians (see figures 2 and 6)

μ outside viscosity

$\hat{\mu}$ inside viscosity

ν outside kinematic viscosity

$\hat{\nu}$ inside kinematic viscosity

ρ ratio of densities, $\frac{\rho'}{\hat{\rho}'}$

ρ' outside density

$\hat{\rho}'$ inside density

σ viscosity ratio, $\frac{\mu}{\hat{\mu}}$

τ dimensionless time parameter, $\frac{U_\infty t_o}{a}$

ϕ potential function

Ψ dimensionless outside stream function, $\frac{\Psi'}{U_\infty\sqrt{\nu t_o}}$

$\hat{\Psi}$ dimensionless inside stream function, $\frac{\hat{\Psi}'}{U_\infty\sqrt{\nu t_o}}$

Ψ' outside stream function, $\int_o^{y'} u'dy'$

$\hat{\Psi}'$ inside stream function, $\int_o^{y'} u'dy'$